Antihormonal-Treatment Status Affects ^{68}Ga-PSMA-HBED-CC PET Biodistribution in Patients with Prostate Cancer

Kilian Kluge[1,2], David Haberl[1,2], Holger Einspieler[1], Sazan Rasul[1], Sebastian Gutschmayer[3], Lukas Kenner[2,4], Gero Kramer[5], Bernhard Grubmüller[5,6,7], Shahrokh Shariat[5,8–12], Alexander Haug[1,2], and Marcus Hacker[1]

[1]*Department of Biomedical Imaging and Image-Guided Therapy, Division of Nuclear Medicine, Medical University of Vienna, Vienna, Austria;* [2]*Christian Doppler Laboratory for Applied Metabolomics, Medical University of Vienna, Vienna, Austria;* [3]*QIMP Team, Medical University of Vienna, Vienna, Austria;* [4]*Department of Pathology, Medical University of Vienna, Vienna, Austria;* [5]*Department of Urology, Medical University of Vienna, Vienna, Austria;* [6]*Department of Urology and Andrology, University Hospital Krems, Krems, Austria;* [7]*Karl Landsteiner University of Health Sciences, Krems, Austria;* [8]*Karl Landsteiner Institute of Urology and Andrology, Vienna, Austria;* [9]*Department of Urology, University of Texas Southwestern Medical Center, Dallas, Texas;* [10]*Division of Urology, Department of Special Surgery, University of Jordan, Amman, Jordan;* [11]*Department of Urology, Second Faculty of Medicine, Charles University, Prague, Czech Republic; and* [12]*Department of Urology, Weill Cornell Medical College, New York, New York*

Androgen deprivation therapy (ADT) is known to influence the prostate-specific membrane antigen (PSMA) expression of prostate cancer, potentially complicating the interpretation of PSMA ligand PET findings and affecting PSMA radioligand therapy. However, the impact of ADT on PSMA ligand biodistribution in nontumorous organs is not well understood. **Methods:** Men (n = 112) with histologically proven prostate cancer who underwent ^{68}Ga-PSMA-HBED-CC (^{68}Ga-PSMA-11) PET/CT between November 2015 and July 2021 at the Medical University Vienna with known ADT status were retrospectively recruited. Fifty-six patients were on gonadotropin-releasing hormone–interfering ADT at the time of imaging (ADT group), whereas 56 patients with no history of ADT served as a control group. Physiologically PSMA-expressing organs (salivary glands, kidneys, liver, and spleen) were delineated, and their uptake was compared according to their data distributions. Multivariate regression analysis assessed the relationship between renal, hepatic, splenic, and salivary gland uptake and the explanatory variables metabolic tumor volume, glomerular filtration rate, and ADT status. **Results:** ADT was associated with lower levels of PSMA uptake in the kidneys (SUV_{mean}: Δ[ADT − control] = −7.89; 95% CI, −10.73 to −5.04; $P < 0.001$), liver (SUV_{peak}: Δ[ADT − control] = −2.3; 95% CI, −5.72 to −0.93; P = 0.003), spleen (SUV_{peak}: Δ[ADT − control] = −1.27; 95% CI, −3.61 to −0.16; P = 0.033), and salivary glands (SUV_{mean}: Δ[ADT − control] = −1.04; 95% CI, −2.48 to −0.13; P = 0.027). In a multivariate analysis, ADT was found to be associated with lower renal (SUV_{mean}: β = −7.95; 95% CI, −11.06 to −4.84; $P < 0.0001$), hepatic (SUV_{peak}: β = −7.85; 95% CI, −11.78 to −3.91; $P < 0.0001$), splenic (SUV_{peak}: β = −5.83; 95% CI, −9.95 to −1.7; P = 0.006), and salivary gland (SUV_{mean}: β = −1.47; 95% CI, −2.76 to −0.17; P = 0.027) uptake. A higher glomerular filtration rate was associated with a higher renal SUV_{mean} (β = 0.16; 95% CI, 0.05 to 0.26; P = 0.0034). **Conclusion:** These findings suggest that ADT systemically modulates PSMA expression, which may have implications for treatment-optimizing and side-effect–minimizing strategies for PSMA radioligand therapies, particularly those using more potent ^{225}Ac-labeled PSMA conjugates.

Key Words: androgen deprivation therapy; prostate cancer; biodistribution; PSMA PET

J Nucl Med 2023; 64:1730–1736
DOI: 10.2967/jnumed.123.265980

Molecular imaging and targeted radioligand therapy (RLT) with prostate-specific membrane antigen (PSMA) ligands have been major diagnostic and therapeutic advances in the management of men with prostate cancer (PCA).

In various preclinical and clinical studies (*1*), the expression of PSMA, a type II membrane glycoprotein found on most PCA cells (*2*) and physiologically on various organs (*3*), has been shown to be modulated by androgen signaling.

Although the exact underlying mechanism remains to be fully elucidated, early work hypothesized that the PSMA enhancer (*4–6*), 1 of 2 crucial regulatory elements of the PSMA gene *FOLH1* (*7*), is, inter alia, inversely and indirectly regulated through sequestration of PSMA enhancer regulating transcription factors (i.e., *SOX, SOX7, SRY*) by activated and nuclear-translocated androgen receptors (*4*).

Since then, various preclinical and clinical studies (*1*) have investigated the effects of androgen deprivation therapy (ADT), a long-established therapeutic cornerstone of PCA management, on PSMA expression of tumorous lesions in an effort to unfold androgen-induced clinical caveats of diagnostic and therapeutic PSMA radioligand use.

Although these studies yielded partly heterogeneous (*8*) and conflicting results (*9*), there is a growing body of evidence suggesting a time-dependent early upregulation (*10,11*) followed by a decrease in PSMA expression of PCA cells after long-term ADT exposure (*12,13*).

Although previous studies focused on ADT influences on tumoral tissue or short-term impact on physiologic PSMA-expressing organs (*14*), literature on physiologic organ uptake after sustained ADT exposure, a commonly encountered clinical scenario in advanced disease before RLT, is currently lacking.

Yet, understanding the influences of ADT on PSMA uptake in nontumorous organs such as the salivary glands and kidneys might have important implications for PSMA RLT, since common side effects such as xerostomia, as well as dose-limiting renal radiotoxicity (*15*), are functions of the PSMA ligand biodistribution.

Received May 3, 2023; revision accepted May 31, 2023.
For correspondence or reprints, contact Marcus Hacker (marcus.hacker@meduniwien.ac.at).
Published online Sep. 21, 2023.

The present study is meant to address this gap in knowledge.

We hypothesized that the PSMA expression of healthy organs would differ in men with PCA depending on their hormonal treatment status.

The objective of this study was to retrospectively compare the ^{68}Ga-PSMA-HBED-CC (^{68}Ga-PSMA-11) PET uptake of the salivary glands, kidneys, liver, and spleen between patients on ADT and patients without any history of ADT.

MATERIALS AND METHODS

Study Design and Cohort Selection

The data of men with histologically proven PCA who underwent ^{68}Ga-PSMA-11 imaging between November 2015 and July 2021 were screened retrospectively.

Patients with conclusive ADT history data were considered for inclusion. Patients on gonadotropin-releasing hormone analogs or antagonists (*16*) during imaging for at least 1 mo or with no history of any ADT were included.

Men on androgen-receptor, 5α-reductase, or CYP17A1 inhibitors were excluded to minimize confounding by heterogeneous treatment regimens.

Scans with metabolic tumor volumes (MTVs) greater than 25 cm^3 were excluded to avoid an influence on ^{68}Ga-PSMA-11 biodistribution by the tumor sink effect (*17*).

All scans were performed after written informed consent was obtained for application of the nonapproved imaging compound ^{68}Ga-PSMA-11, and the need for written informed consent for retrospective data collection and analysis was waived (ethics committee identification number 1745/2021).

The primary endpoint of this study was the SUV_{mean} and SUV_{peak} of organs with physiologic PSMA expression, namely the submandibular glands, kidneys, liver, and spleen. The secondary endpoints were the SUV_{mean} of organs according to midterm (1–6 mo) and long-term (>6 mo) ADT exposure when the primary endpoint was met.

Imaging Protocol

All scans were obtained on a Biograph TruePoint PET/CT scanner (Siemens Healthineers). The patients were intravenously injected with a mean of 182.6 MBq (±18.7 [SD]) of ^{68}Ga-PSMA-11. Sixty minutes after injection, static, whole-body scans were obtained from the skull base to the upper femur. First, CT scans were acquired at 120 kV and 230 mAs with intravenous contrast medium (CT matrix size, 512 × 512) unless contraindications for contrast application existed. Afterward, PET scans were acquired at 3–4 bed positions, reconstructed iteratively using a point-spread-function–based algorithm, and subsequently corrected for scatter and attenuation on the basis of the CT scan (PET matrix size, 168 × 168).

Image Analysis

Physiologically PSMA-expressing organs were assessed, namely the submandibular glands, kidneys, liver, and spleen. The submandibular glands were chosen as a surrogate for overall salivary gland PSMA uptake since they were fully included in most fields of view (except in 2 scans). The organs were delineated in a 2-step process. First, the deep-learning–based Multi-Organ Objective Segmentation framework (*18*) was used to obtain CT-defined organ delineations of the liver, spleen, and kidneys. Next, the framework-derived segmentations were reviewed and, if necessary, adjusted manually to the PET component using Slicer3D software (version 4.11) (*19*) by a nuclear medicine physician. The submandibular glands were delineated on the PET component using the semiautomated Slicer3D extension PETTumorSegmentation (*20*). Two nuclear medicine physicians delineated tumor lesions manually on a dedicated workstation using Hybrid 3D software (version 4.17; Hermes Medical Solutions). SUV_{mean} and SUV_{peak} not corrected for lean body mass and MTV were extracted from the regions of interest.

Statistical Analysis

Numeric variables were expressed as mean (±SD), and discrete outcomes were expressed as absolute (*n*) and relative (%) frequencies. The group comparability of the control and ADT groups was assessed by comparing baseline demographic data. The normality and heteroskedasticity of continuous data were assessed with the Shapiro–Wilk and Levene tests, respectively. Continuous outcomes were compared using the unpaired Student *t* test, Welch *t* test, and Mann–Whitney *U* test according to the data distribution. Discrete outcomes were compared using the χ^2 or Fisher exact test accordingly. All tests were 2-tailed.

Statistical tests for differences in visceral organ metastasis PSMA uptake could not be computed because of the sample size ($n = 1$ in the ADT group).

Differences between renal, hepatic, splenic, and salivary gland uptake were assessed according to prior cytotoxic treatments with chemotherapy or ^{177}Lu-PSMA RLTs.

Additionally, differences between renal, hepatic, splenic, and salivary gland PSMA uptake were assessed according to midterm (1–6 mo) and long-term (>6 mo) ADT runtimes with ANOVA and the Kruskal–Wallis test according to the data distribution. If the null hypothesis of the ANOVA and the Kruskal–Wallis test was rejected, post hoc pairwise analyses were performed with the Tukey honestly significant difference test and the Dunn–Bonferroni test, respectively.

Multivariate Regression Analysis

Multivariate regression analysis was performed to assess the relationship between renal and salivary gland SUV_{mean}, as well as the relationship of hepatic and splenic SUV_{peak} with the following explanatory variables: MTV, glomerular filtration rate, and ADT status. Data were checked for multicollinearity with the Belsley–Kuh–Welsch technique. The heteroskedasticity and normality of residuals were assessed by, respectively, the Breusch–Pagan test and the Shapiro–Wilk test. The α-risk was set for all statistical analyses to 5% ($\alpha = 0.05$).

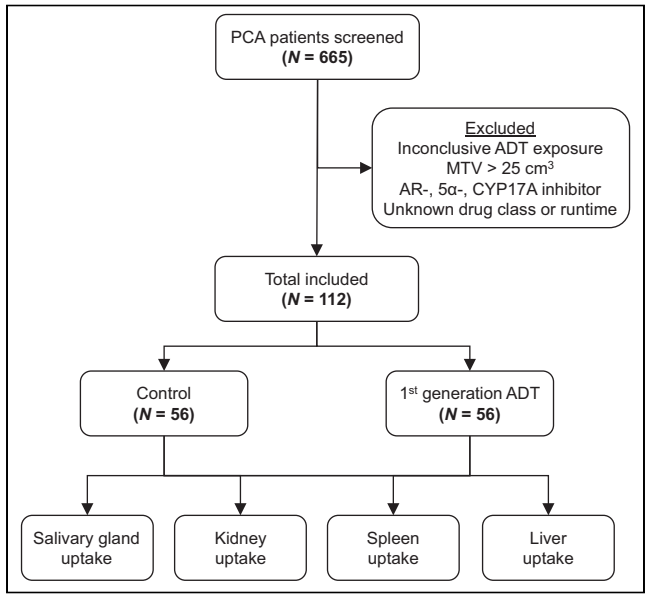

FIGURE 1. CONSORT (Consolidated Standards of Reporting Trials) diagram. AR = androgen receptor; 5α- = 5α-reductase.

Statistical analysis was performed with EasyMedStat software (version 3.24; EasyMedStat).

RESULTS

Clinical Cohort

Of 665 screened men with PCA and available PSMA PET/CT, 112 (17%) with a conclusive ADT treatment history at the time of imaging were entered into this study according to the inclusion criteria (Fig. 1). The demographic and clinical characteristics are summarized in Table 1.

Organ PSMA Uptake Measurements

Differences in organ uptake between the ADT and control groups are summarized in Table 2.

There was a significantly lower mean renal SUV_{mean} (Δ[ADT − control] = −7.89; 95% CI, −10.73 to −5.04; $P < 0.001$) and SUV_{peak} (Δ[ADT − control] = −14.12; 95% CI, −19.85 to −8.39; $P < 0.001$) in the ADT group than in the control group. Similarly, median hepatic SUV_{peak} (Δ[ADT − control] = −2.3; 95% CI, −5.72 to −0.93; $P = 0.003$), median splenic SUV_{peak} (Δ[ADT − control] = −1.27; 95% CI, −3.61 to −0.16; $P = 0.033$), and median salivary gland SUV_{mean} (Δ[ADT − control] = −1.04; 95% CI, −2.48 to −0.13; $P = 0.027$) and mean SUV_{peak} (Δ[ADT − control] = −3.31; 95% CI, −5.3 to −1.31; $P = 0.001$) were significantly lower in the ADT group (Fig. 2).

Secondary Endpoint Analysis According to ADT Runtime Length

The mean renal SUV_{mean} was 29.5 (SD, 7.2), 21.6 (SD, 8.37), and 21.61 (SD, 7.61) for the control group, patients on 1–6 mo of

TABLE 1
Demographic and Clinical Patient Data

Variable	Control ($n = 56$)	ADT ($n = 56$)	*P*
Age (y)	69.6 (±7.2)	70.4 (±8.0)	0.58
Weight (kg)	86.2 (±12.6)	83.4 (±13.6)	0.31
Tracer dose (MBq)	181.8 (±18.1)	183.4 (±19.4)	0.59
PSA (μg/dL)*	13.0 (±46.1)	7.1 (±12.6)	0.06
GFR (mL/min)†	78.4 (±15.5)	81.0 (±14.2)	0.39
MTV (cm^3)	3.3 (±5.3)	5.0 (±6.2)	0.20
PSMA-positive lesions			
Prostate	21 (37.5%)	21 (37.5%)	>0.99
Lymph nodes	19 (33.9%)	14 (25.0%)	0.41
Bone	8 (14.3%)	18 (32.1%)	0.04
Viscera (lung)	2 (3.6%)	1 (1.8%)	>0.99
Mean lesional SUV_{mean}			
Prostate	13.1 (±11.4)	10.8 (±8.4)	0.43
Lymph nodes	7.5 (±4.3)	10.39 (±6.3)	0.13
Bone	4.9 (±2.2)	9.4 (±12.5)	0.84
Viscera (lung)	4.79 (4.0–5.6)	7.7	—‡
Mean ADT runtime (m)	—	24.0 ± 34.9	
Runtimes binned (m)			
1–6	—	15 (26.8%)	
>6	—	41 (73.2%)	
ADT drug class			
GnRH analog			
Leuprorelin	—	38 (67.9%)	
Triptorelin	—	2 (3.6%)	
GnRH antagonist			
Degarelix	—	16 (28.6%)	
Previous cytotoxic treatments		20 (35.7%)	
CHT	—	19 (33.9%)	
^{177}Lu-PSMA	—	3 (5.3%)	

*Missing data for control ($n = 8$) and ADT group ($n = 4$).
†Missing data for control ($n = 9$) and ADT group ($n = 8$).
‡Statistical testing not feasible because of sample size in control group ($n = 2$; data as mean and range) and ADT group ($n = 1$).
PSA = prostate-specific antigen; GFR = glomerular filtration rate; GnRH = gonadotropin-releasing hormone; CHT = chemotherapy.
Qualitative data are number and percentages; continuous data are mean and SD.

TABLE 2
PSMA Uptake Levels of Normal Organs According to Antihormonal Treatment Status

Variable	Control (n = 56)	ADT (n = 56)	Difference	P
Kidney SUV_{mean}*†	29.5 ± 7.2; 95% CI, 27.57–31.42; range, 16.59–52.12	21.61 ± 8.1; 95% CI, 19.44–23.78; range, 5.18–37.36	Δyes − no = −7.89; 95% CI, −10.73 to −5.04	<0.001
Kidney SUV_{peak}*	54.76 ± 14.29; 95% CI, 50.94–58.59; range, 26.65–93.75	40.64 ± 16.49; 95% CI, 36.23–45.06; range, 6.82–77.99	Δyes − no = −14.12; 95% CI, −19.85 to −8.39	<0.001
Liver SUV_{mean}‡	4.8 ± 1.31; 95% CI, 4.45–5.15; range, 2.15–8.63	4.44 ± 1.65; 95% CI, 3.99–4.88; range, 0.92–10.39	ΔADT − control = −0.14; 95% CI, −0.86 to 0.10	0.12
Liver SUV_{peak}‡	18.06 ± 14.75; 95% CI, 14.11–22.01; range, 3.81–55.8	11.18 ± 8.97; 95% CI, 8.78–13.58; range, 1.19–37.64	ΔADT − control = −2.3; 95% CI, −5.72 to −0.93	0.003
Spleen SUV_{mean}‡	6.08 ± 2.04; 95% CI, 5.53–6.62; range, 2.55–11.59	5.86 ± 2.42; 95% CI, 5.21–6.51; range, 0.782–14.56	Δyes − no = −0.49; 95% CI, −1.5 to 0.99	0.46
Spleen SUV_{peak}‡	14.76 ± 11.15; 95% CI, 11.78–17.75; range, 4.81–53.79	11.56 ± 9.61; 95% CI, 8.99–14.13; range, 1.14–52.34	ΔADT − control = −1.27; 95% CI, −3.61 to −0.16	0.033
Salivary gland SUV_{mean}‡§	11.34 ± 2.69; 95% CI, 10.62–12.06; range, 4.41–17.05	9.93 ± 3.17; 95% CI, 9.07–10.8; range, 1.18–18.02	ΔADT − control = −1.04; 95% CI, −2.48 to −0.13	0.027
Salivary gland SUV_{peak}*	20.0 ± 5.02; 95% CI, 18.65–21.34; range, 7.53–34.76	16.69 ± 5.61; 95% CI, 15.16–18.22; range, 1.7–30.42	ΔADT − control = −3.31; 95% CI, −5.3 to −1.31	0.001

*t test data as mean ± SD.
†Two patients underwent unilateral nephrectomy.
‡Mann–Whitney test data as median and IQR.
§Two scans (2/56, 4%) did not include salivary glands in field of view.

ADT, and patients on more than 6 mo of ADT, respectively (P < 0.001). Post hoc pairwise analysis revealed significant differences between the control group and the 1- to 6-mo ADT group (mean difference: 95% CI, −13.2 to −2.56; P = 0.002) and between the control group and the group receiving more than 6 mo of ADT (95% CI, −11.65 to −4.13; P < 0.001). No significant difference between the 2 ADT groups was observed (95% CI, −5.51 to 5.53; P > 0.999).

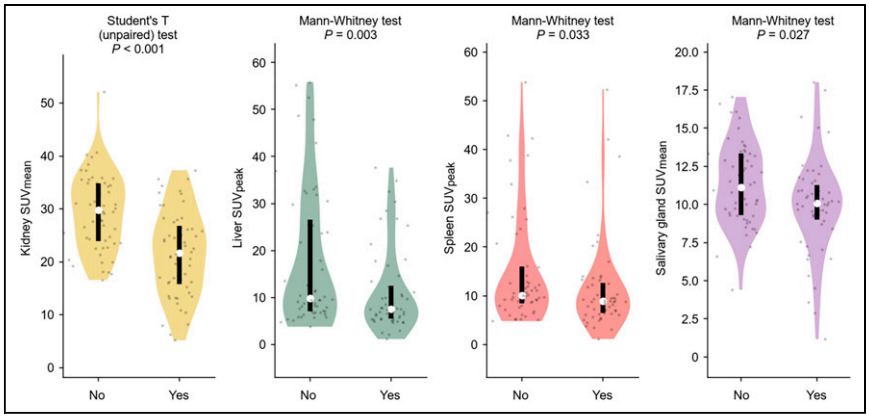

FIGURE 2. Violin plots of significantly different exemplary PSMA uptake levels of normal organs according to ADT treatment status. White dots indicate median value. No = control; Yes = ADT.

The median hepatic SUV_{peak} was 9.9 (interquartile range [IQR], 19.43), 6.64 (IQR, 8.74), and 7.61 (IQR, 5.17) in the control group, the group receiving 1–6 mo of ADT, and the group receiving more than 6 mo of ADT, respectively (P = 0.012). After post hoc adjustment, only the difference between the control group and the group receiving more than 6 mo of ADT remained significant (95% CI, −13.46 to −1.07; P = 0.006).

The mean salivary gland SUV_{mean} was 11.34 (SD, 2.69), 10.2 (SD, 3.8), and 9.83 (SD, 2.94) for the control group, the group receiving 1–6 mo of ADT, and the group receiving more than 6 mo of ADT, respectively (P = 0.043). Pairwise analysis showed significant differences between the control group and the group receiving more than 6 mo of ADT (95% CI, −2.97 to −0.053; P = 0.041) (Fig. 3).

Subgroup Analysis of ADT Group According to Previous Systemic Treatments

There was no statistical difference in mean renal or salivary gland SUV_{mean} or median hepatic or splenic SUV_{peak} between patients who underwent prior additional systemic therapies, namely taxane-based

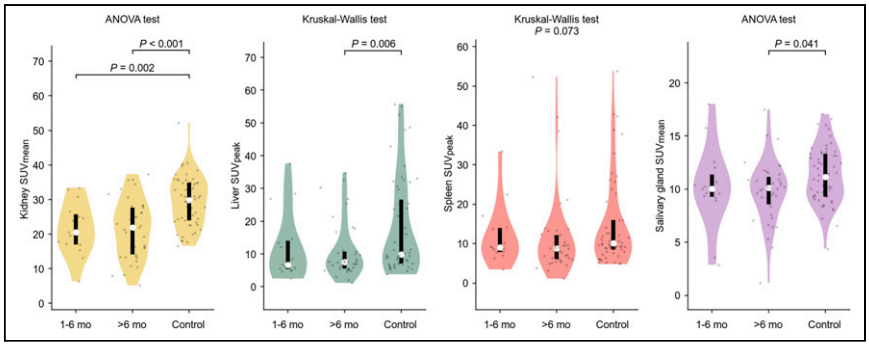

FIGURE 3. Violin plots of PSMA uptake levels of normal organs in ADT group according to different ADT runtimes and control group. Only significant values after post hoc testing are displayed as bars on figures. Nonsignificant *P* values are displayed in figure heading. White dots indicate median values.

chemotherapies, ^{177}Lu-PSMA-617, or I&T RLT (24.93 [SD, 6.82], 10.02 [SD, 2.01], 7.8 [IQR, 6.16], and 8.54 [IQR, 2.96], respectively) and patients who did not receive prior additional systemic therapies (25.69 [SD, 8.97], 10.79 [SD, 3.18], 8.82 [IQR, 17.47], and 9.72 [IQR, 6.36], respectively) (Fig. 4).

Multivariate Analysis of PSMA Organ Uptake

In the multivariate analysis, ADT was identified as an independent predictor of lower renal SUV_{mean} ($\beta = -7.95$; 95% CI, −11.06 to −4.84; $P < 0.0001$), hepatic SUV_{peak} ($\beta = -7.85$; 95% CI, −11.78 to −3.91; $P < 0.0001$), splenic SUV_{peak} ($\beta = -5.83$; 95% CI, −9.95 to −1.7; $P = 0.0062$), and salivary glandular SUV_{mean} ($\beta = -1.47$; 95% CI, −2.76 to −0.17; $P = 0.0274$). In addition, a high glomerular filtration rate was predictive only of a high renal SUV_{mean} ($\beta = 0.16$; 95% CI, 0.05 to 0.26; $P = 0.0034$) (Table 3).

DISCUSSION

This study presents the first evidence that PCA patients on sustained ADT exhibit significantly lower ^{68}Ga-PSMA-11 uptake in the salivary glands, liver, spleen, and kidneys than do hormonal therapy-naïve patients.

Although it is widely appreciated that ADT influences the PSMA expression of cancerous lesions, most likely in a time-dependent dichotomous manner (*1*), the effect of ADT on physiologically PSMA-expressing organs such as the salivary glands, kidneys, liver, and spleen has been assessed only in a short-term setting (*14*).

This report therefore advances our understanding of the physiologic PSMA biodistribution in patients on sustained ADT and corroborates earlier findings (*14*) that hormonal changes exert a systemic influence on PSMA expression also in nontumorous tissues, holding possible implications for optimization strategies for PSMA RLTs.

Ettala et al. (*14*) investigated the short-term (pretreatment till a maximum of 8 wk after initiation) time-course effect of gonadotropin-releasing hormone–modulating ADT on the ^{68}Ga-PSMA-11 SUV_{max} of cancer lesions and physiologic PSMA-avid organs (salivary glands, kidneys, liver, and spleen) in newly diagnosed men with high-risk PCA ($n = 9$) and observed heterogeneous and time-dependent uptake changes in tumorous and nontumorous tissues alike. Although they observed an initial heterogeneous uptake increase in all physiologically PSMA-avid organs, which peaked at around week 4, most patients who continued imaging beyond 1 mo started exhibiting stabilizing or falling PSMA organ uptake trajectories, which were most pronounced in the salivary glands and kidneys.

Analogously, several authors (*12,21*) have reported decreasing PSMA expression in tumorous lesions after long-term exposure to different classes of ADT. Although Vallabhajosula et al. (*21*) observed an initial increase in PSMA-expressing PCA lesions after 2 wk of abiraterone or enzalutamide ($n = 4$), followed by a decrease in uptake after 3 mo, Afshar-Oromieh et al. (*12*) reported decreased PSMA uptake in roughly two thirds of PCA lesions after sustained gonadotropin-releasing hormone antagonist or analog exposure (median ADT runtime, ∼7 mo) in a retrospective, longitudinal cohort of 10 patients.

In summary with the abovementioned studies (*12,14,21*), the found association between midterm or, predominantly, long-term ADT and significantly lower PSMA uptake in the submandibular glands, liver, spleen, and kidneys (Fig. 3) suggests that not just tumorous but also nontumorous tissues might be subject to androgen-induced, time-dependent, dichotomous PSMA expression changes in early upregulation and late downregulation (*1*).

Surprisingly, we did not observe any PSMA uptake level differences of cancerous lesions between patients on ADT and those without a history of ADT, as repeatedly reported in the literature (*10–12*). We hypothesize that this might be due to the cross-sectional study design incorporating patients at different stages. Although patients on ADT have more advanced disease (*22*), as signified by a higher number of osseous bone lesions on imaging, the reported effects of hormonal therapy on cancer lesions could be blurred by ADT-induced PSMA downregulation of yet more advanced lesions in our cohort.

Since PSMA biodistribution in itself is a complex function of uptake, retention,

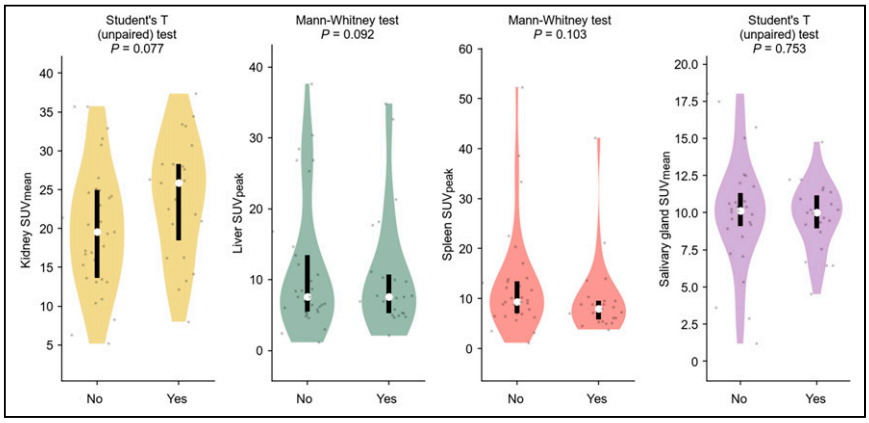

FIGURE 4. Violin plots of PSMA uptake levels according to prior cytotoxic treatments (^{177}Lu-PSMA RLT or chemotherapy) in normal organs. White dots indicate median value. Yes = prior systemic therapies; No = no prior systemic therapy.

TABLE 3
Multivariate Regression Analysis of Relationship Between Renal, Hepatic, Splenic, and Salivary Gland PSMA Uptake and Explanatory Variables MTV, Glomerular Filtration Rate, and ADT Status

Predicted endpoint	Variable	Odds ratio	*P*
Kidney SUV_{mean}			
	Intercept	17.78; 9.28 to 26.27	<0.0001
	MTV (cm^3)	−0.218; −0.495 to 0.0585	0.121
	GFR (mL/min)	0.156; 0.0531 to 0.259	0.0034
	ADT (0 = no, 1 = yes)	−7.95; −11.06 to −4.84	<0.0001
Liver SUV_{peak}			
	Intercept	10.94; −1.06 to 22.94	0.0735
	MTV (cm^3)	0.0389; −0.301 to 0.379	0.821
	GFR (mL/min)	0.09; −0.0606 to 0.241	0.238
	ADT (0 = no, 1 = yes)	−7.85; −11.78 to −3.91	<0.0001
Spleen SUV_{peak}			
	Intercept	6.36; −5.73 to 18.45	0.299
	MTV (cm^3)	0.295; −0.114 to 0.704	0.156
	GFR (mL/min)	0.104; −0.0615 to 0.27	0.214
	ADT (0 = no, 1 = yes)	−5.83; −9.95 to −1.7	0.006
SM SUV_{mean}			
	Intercept	12.2; 8.67 to 15.73	<0.0001
	MTV (cm^3)	−0.0679; −0.183 to 0.0472	0.244
	GFR (mL/min)	−0.00771; −0.0506 to 0.0352	0.722
	ADT (0 = no, 1 = yes)	−1.47; −2.76 to −0.167	0.0274

GFR = glomerular filtration rate; SM = Submandibular gland.
Odds ratio is followed by 95% CI.

and excretion (*17,23*) in tumorous and nontumorous tissues, a multivariate regression analysis was performed to exclude the confounding effects of renal function and tumor tissue.

The MTV was not associated with salivary gland, hepatic, splenic, or renal uptake in the ADT group, most likely since the potential influence of the tumor sink effect (*17*), a sequestration phenomenon that occurs when extensive tumor masses reduce tracer accumulation in healthy tissues, was excluded by design (Fig. 1).

Interestingly, renal function was positively associated with renal PSMA uptake levels. We hypothesize that although there is a physiologic renal baseline PSMA expression, primarily in the proximal tubular cells (*3*), increased PSMA excretion in the case of higher glomerular filtration led to higher overall renal radioligand signal caused by count summation during static image acquisition.

Since sustained ADT is a commonly encountered clinical scenario in patients with advanced disease, a deeper understanding of the hormonal influences on PSMA biodistribution might have important implications for PSMA RLTs because common side effects, such as xerostomia and dose-limiting renal radiotoxicity (*15*), are functions of PSMA ligand biodistribution.

Even though dosimetric estimates of absorbed organ doses are the gold standard, ^{68}Ga-PSMA-11 PET has been shown to provide robust estimates of therapeutic PSMA ligand biodistributions (*24,25*) in that regard.

Our study had several limitations, and the findings should therefore be interpreted with caution.

First, as a retrospective, cross-sectional, and monocentric study, it was prone to selection bias, recall bias, inaccuracies in record keeping, and incomplete data, which could negatively affect the generalizability of the findings. We tried to minimize this potential bias by focusing on a narrow definition of ADT treatment and including only patients with complete hormonal treatment data, as well as by ensuring balanced groups according to possible confounders such as renal function, MTV (*17*), and previous systemic treatments (Fig. 4). Furthermore, multivariate regression analysis was performed to discover potential confounders, which, however, cannot fully be excluded.

Second, as a cross-sectional study, no causal relationships can be inferred. However, a cross-sectional study is a suitable design to assess nontemporal relationships between variables and to generate hypotheses. Therefore, we envision that groups with longitudinal or dosimetric datasets are able to establish a cause–effect relationship between gonadotropin-releasing hormone–modulating ADT and more potent antiandrogens such as androgen receptor inhibitors, 5α-reductase, and CYP17a inhibitors on the PSMA biodistribution, as an understanding of hormonal influences might have important implications for efficacy-maximizing and side-effect–minimizing strategies for RLT.

CONCLUSION

These findings suggest that long-term ADT modulates PSMA expression in a systemic fashion, which may have implications for

treatment-optimizing and side-effect–minimizing strategies for PSMA RLTs. Further, longitudinal studies also incorporating second-generation ADT are warranted to establish a cause–effect relationship and effect magnitude.

DISCLOSURE

This study was partially funded by the Austrian Federal Ministry for Digital and Economic Affairs; the National Foundation for Research, Technology, and Development; the Christian Doppler Research Association; and Siemens Healthineers. No other potential conflict of interest relevant to this article was reported.

KEY POINTS

QUESTION: Is ADT associated with the biodistribution of ^{68}Ga-PSMA-11?

PERTINENT FINDINGS: In this monocentric, retrospective study, the ^{68}Ga-PSMA-11 uptake of physiologically PSMA-avid organs was compared between patients on midterm and long-term ADT ($n = 56$) and a control group ($n = 56$). The ADT cohort had significantly lower PSMA uptake in the salivary glands, liver, spleen, and kidneys.

IMPLICATIONS FOR PATIENT CARE: These findings suggest that long-term ADT modulates PSMA expression in a systemic fashion, which may have implications for treatment-optimizing and side-effect–minimizing strategies for PSMA RLTs, particularly those using more potent ^{225}Ac-labeled PSMA conjugates.

REFERENCES

1. Vaz S, Hadaschik B, Gabriel M, Herrmann K, Eiber M, Costa D. Influence of androgen deprivation therapy on PSMA expression and PSMA-ligand PET imaging of prostate cancer patients. *Eur J Nucl Med Mol Imaging.* 2020;47:9–15.
2. Sweat SD, Pacelli A, Murphy GP, Bostwick DG. Prostate-specific membrane antigen expression is greatest in prostate adenocarcinoma and lymph node metastases. *Urology.* 1998;52:637–640.
3. Uhlén M, Fagerberg L, Hallström BM, et al. Proteomics. Tissue-based map of the human proteome. *Science.* 2015;347:1260419.
4. Ghosh A, Heston WDW. Tumor target prostate-specific membrane antigen (PSMA) and its regulation in prostate cancer. *J Cell Biochem.* 2004;91:528–539.
5. Watt F, Martorana A, Brookes DE, et al. A tissue-specific enhancer of the prostate-specific membrane antigen gene, FOLH1. *Genomics.* 2001;73:243–254.
6. Noss KR, Wolfe SA, Grimes SR. Upregulation of prostate-specific membrane antigen/folate hydrolase transcription by an enhancer. *Gene.* 2002;285:247–256.
7. O'Keefe DS, Bacich DJ, Heston WDW. Prostate specific membrane antigen. In: Chung LWK, Isaacs WB, Simons JW, eds. *Prostate Cancer: Biology, Genetics, and the New Therapeutics.* Humana Press; 2001:307–326.
8. Aggarwal R, Wei X, Kim W, et al. Heterogeneous flare in prostate-specific membrane antigen positron emission tomography tracer uptake with initiation of androgen pathway blockade in metastatic prostate cancer. *Eur Urol Oncol.* 2018;1:78–82.
9. Chang SS, Reuter VE, Heston WD, Hutchinson B, Grauer LS, Gaudin PB. Short-term neoadjuvant androgen deprivation therapy does not affect prostate-specific membrane antigen expression in prostate tissues. *Cancer.* 2000;88:407–415.
10. Emmett L, Yin C, Crumbaker M, et al. Rapid modulation of PSMA expression by androgen deprivation: serial ^{68}Ga-PSMA-11 PET in men with hormone-sensitive and castrate-resistant prostate cancer commencing androgen blockade. *J Nucl Med.* 2019;60:950–954.
11. Hope TA, Truillet C, Ehman EC, et al. ^{68}Ga-PSMA-11 PET imaging of response to androgen receptor inhibition: first human experience. *J Nucl Med.* 2017;58:81–84.
12. Afshar-Oromieh A, Debus N, Uhrig M, et al. Impact of long-term androgen deprivation therapy on PSMA ligand PET/CT in patients with castration-sensitive prostate cancer. *Eur J Nucl Med Mol Imaging.* 2018;45:2045–2054.
13. Liu T, Wu LY, Fulton MD, Johnson JM, Berkman CE. Prolonged androgen deprivation leads to downregulation of androgen receptor and prostate-specific membrane antigen in prostate cancer cells. *Int J Oncol.* 2012;41:2087–2092.
14. Ettala O, Malaspina S, Tuokkola T, et al. Prospective study on the effect of short-term androgen deprivation therapy on PSMA uptake evaluated with ^{68}Ga-PSMA-11 PET/MRI in men with treatment-naïve prostate cancer. *Eur J Nucl Med Mol Imaging.* 2020;47:665–673.
15. Okamoto S, Thieme A, Allmann J, et al. Radiation dosimetry for ^{177}Lu-PSMA I&T in metastatic castration-resistant prostate cancer: absorbed dose in normal organs and tumor lesions. *J Nucl Med.* 2017;58:445–450.
16. Crawford ED, Schellhammer PF, McLeod DG, et al. Androgen receptor targeted treatments of prostate cancer: 35 years of progress with antiandrogens. *J Urol.* 2018;200:956–966.
17. Gafita A, Wang H, Robertson A, et al. Tumor sink effect in ^{68}Ga-PSMA-11 PET: myth or reality? *J Nucl Med.* 2022;63:226–232.
18. Shiyam Sundar LK, Yu J, Muzik O, et al. Fully automated, semantic segmentation of whole-body 18F-FDG PET/CT images based on data-centric artificial intelligence. *J Nucl Med.* 2022;63:1941–1948.
19. Fedorov A, Beichel R, Kalpathy-Cramer J, et al. 3D Slicer as an image computing platform for the Quantitative Imaging Network. *Magn Reson Imaging.* 2012;30:1323–1341.
20. Beichel RR, Van Tol M, Ulrich EJ, et al. Semiautomated segmentation of head and neck cancers in ^{18}F-FDG PET scans: a just-enough-interaction approach. *Med Phys.* 2016;43:2948–2964.
21. Vallabhajosula S, Jhanwar Y, Tagawa S, et al. ^{99m}Tc-MIP-1404 planar and SPECT scan: imaging biomarker of androgen receptor (AR) signaling and prostate specific membrane antigen (PSMA) expression [abstract]. *J Nucl Med.* 2016;57(suppl 2):1541.
22. Afshar-Oromieh A, Avtzi E, Giesel FL, et al. The diagnostic value of PET/CT imaging with the ^{68}Ga-labelled PSMA ligand HBED-CC in the diagnosis of recurrent prostate cancer. *Eur J Nucl Med Mol Imaging.* 2015;42:197–209.
23. Pfob CH, Ziegler S, Graner FP, et al. Biodistribution and radiation dosimetry of ^{68}Ga-PSMA HBED CC: a PSMA specific probe for PET imaging of prostate cancer. *Eur J Nucl Med Mol Imaging.* 2016;43:1962–1970.
24. Wang J, Zang J, Wang H, et al. Pretherapeutic ^{68}Ga-PSMA-617 PET may indicate the dosimetry of ^{177}Lu-PSMA-617 and ^{177}Lu-EB-PSMA-617 in main organs and tumor lesions. *Clin Nucl Med.* 2019;44:431–438.
25. Violet J, Jackson P, Ferdinandus J, et al. Dosimetry of Lu-PSMA-617 in metastatic castration-resistant prostate cancer: correlations between pretherapeutic imaging and whole-body tumor dosimetry with treatment outcomes. *J Nucl Med.* 2019;60:517–523.